Ionic Transport in Lipid Bilayer Membranes

F. Bordi,* C. Cametti,# and A. Naglieri#

*Sezione di Fisica Medica, Dipartimento di Medicina Interna, Universita' di Roma "Tor Vergata," and Istituto Nazionale di Fisica della Materia (INFM), Unita' di Roma I, and #Dipartimento di Fisica, Universita' di Roma "La Sapienza," and Istituto Nazionale di Fisica della Materia (INFM), Unita' di Roma I, Rome, Italy

ABSTRACT The current-voltage relationships of model bilayer membranes have been measured in various phospholipid systems, under the influence of both a gradient of potential and an ionic concentration, in order to describe the ion translocation through hydrated transient defects (water channels) across the bilayer formed because of lipid structure fluctuations and induced by temperature. The results have been analyzed in the light of a statistical rate theory for the transport process across a lipid bilayer, recently proposed by Skinner et al. (1993). In order to take into account the observed I-V curves and in particular the deviation from an ohmic behavior observed at high potential values, the original model has been modified, and a new version has been proposed by introducing an additional kinetic process. In this way, a very good agreement with the experimental values has been obtained for all of the systems we have investigated (dimyristoylphosphatidyl ethanolamine bilayers and mixed systems composed by dimyristoylphosphatidyl ethanolamine/dimyristoylphosphatidylcholine mixtures and dimyristoylphosphatidyl ethanolamine/phosphatidic acid dipalmitoyl mixtures). The rate constants governing the reactions at the bilayer interfaces have been evaluated for K^+ and Cl^- ions, as a function of temperature, from 5 to 35°C and bulk ionic concentrations from 0.02 to 0.2 M. Finally, a comparison between the original model of Skinner and the modified version is presented, and the advantages of this new formulation are briefly discussed.

INTRODUCTION

Phospholipid bilayer membranes represent a useful model system to investigate basic aspects of the lipid bilayer components of biological cell membranes and, particularly, to study the passive ionic transport processes.

Although the electrical properties of lipid bilayers, which are of fundamental importance in many areas of biology (Weiss, 1996), have been intensely characterized by means of different experimental techniques (Hianik and Passechnik, 1995; Cevc and Marsh, 1987), the basic mechanism of the ion translocation and ion permeation responsible for the observed, relatively low conductance is not yet completely understood, and various sophisticated models have been proposed (Levitt, 1986; Schumaker and MacKinnon, 1990; Läuger, 1976; Levitt, 1991; Hladky, 1992). This is primarily because of both the difficulty of characterizing, from an electrical point of view, the lipid bilayer and the fact that the electrical conductance reflects different averaged processes at a macroscopic level. All of them are strongly dependent on the physical-chemical conditions, such as ionic strength and pH of the aqueous solvent, temperature, besides the structural arrangement of the hydrophobic lipid matrix.

In the simplest version of the transport model of ions in layered or confined structures, ions must diffuse up to the membrane, adsorb, cross the membrane core, desorb, and finally diffuse away on the other side of the membrane itself. Among these different steps describing the overall transport of an ion across the lipid membrane, the adsorbing and desorbing processes are particularly dependent on the potential barrier at the interfaces and voltage drops in the polar and nonpolar regions and on the structure of the double layer at the surface of the charged membrane. In addition, the ion migration through the membrane core cannot be explained only by Born energy, around 100 kJ/mol (Parsegian, 1969; Deamer and Nichols, 1989; Smith et al., 1984; Lasic, 1993), which predicts ionic fluxes of three or more orders of magnitude lower than those observed experimentally.

In contrast to some nonelectrolytes, the flux of cations and, to a lesser extent, anions can be qualitatively justified by a diffusion process through statistically created pores, i.e., the formation of short-lived, water-filled structures as a consequence of statistical fluctuations in the lipid organization that allow ions to pass throughout the bilayer. Mechanisms that suggest that ion permeation across a lipid membrane could occur through hydrated transient defects produced by thermal fluctuation have been recently proposed by different authors (Nichols and Deamer, 1980; Bhowmik and Nandy, 1983; Lawaczeck, 1988; Jansen and Blume, 1995; Paula et al., 1996). As pointed out by Smith et al. (1984), these pores could be formed because of fluctuations in the lipid organization, but their density order of 10^6-10^7 pores/cm^2 (Smith et al., 1984) is sufficiently small to unaffect the basic structure of the hydrophobic region of the lipid bilayer.

In fact, the cooperative nature of the membrane assembly imparts the bilayer with a considerable degree of dynamic heterogeneity that is believed to favor the formation of water channels (pores) along which ions can diffuse. These microscopic domains, induced by thermal density fluctuations, persist on a time scale of typically 10^{-6}-10^{-7} s,

Received for publication 7 April 1997 and in final form 19 November 1997.

Address reprint requests to Dr. C. Cametti, Dipartimento di Fisica, Universita' di Roma "La Sapienza," Piazzale A. Moro 2, 00185 Rome, Italy. Tel.: 39-6-49913476; Fax: 39-6-4463158; E-mail: cesare.cametti@roma1.infn.it.

0006-3495/98/03/1358/13 $2.00

provide for highly effective transfer of ions across the bilayer, and greatly reduce the electrostatic transfer energy (Born energy) associated with moving ions from an aqueous phase to the hydrocarbon interior of the lipid bilayer.

These heterogeneities are also present in biological cell membranes (Lipowski and Sackmann, 1995) in which they are important for many cell functions and serve as fundamental elements through which small anions, cations, and other polar solutes, besides water, cross the membrane and make possible the cell volume regulation. In this context, a pore is viewed as an hole that offers to the ion an hydrophilic pathway through which it can diffuse across the apolar core of the lipid bilayer, and the membrane structure, as a whole, can be considered as a metastable system in which, as a result of heat fluctuations, pores of appropriate radius and lifetimes can be formed.

The change in the membrane free energy during the formation of a pore of radius r can be written, to a first approximation, as (Chizmadzhev, 1988)

$$\Delta F = -\pi r^2\sigma + 2\pi r\gamma - \pi r^2 C_m(\epsilon_m\epsilon_p - 1)V^2/2$$

in which σ and γ are the bilayer tension and the pore linear tension, ϵ_m and ϵ_p are the permittivities of aqueous and hydrophobic phase, respectively, C_m is the specific capacitance, and V is the total potential difference applied to the bilayer. Owing to the parabolic dependence of the free energy on the radius r, the above equation shows that once the size of a pore exceeds a particular value r_o

$$r_0 = \frac{\gamma}{\sigma + C_m(\epsilon_m\epsilon_p - 1)V^2 2}$$

the radius r begins to increase. Moreover, the work of the pore formation (the height of the potential barrier) decreases with the increase of the applied potential, thus resulting in a reduction of the critical pore radius. These two effects contribute to stabilize the pore distribution when the tension γ is made dependent on the pore radius, and the hydrational repulsion between pore edges is considered.

Evidence in favor of this idea is provided by electroporation experiments leading to membrane fusion (Chizmadzhev, 1988) or by conductance jumps (Antonov et al., 1980; Kaufmann and Silman, 1983; Vyshenskaia and Pasechnik, 1986) observed during lipid phase transitions and finally by computer models of lipid dynamics in bilayers (Owenson and Pratt, 1984). Recently, measurements of permeation of small ions and other small polar molecules through phospholipid bilayers (Paula et al., 1996) also confirm that pores are the dominant mechanism to the diffusion of ions.

These findings support the idea that the hydrophobic region of a lipid bilayer does not behave as a uniform phase, but it is the seat of transient fluctuations that allow ionic conductance at an higher rate than that predicted by Born energy considerations.

In this study, we investigated the ionic flux across a lipid bilayer, which takes both ion concentration and electrical potential gradients into account as driving forces, following a statistical rate theory approach recently proposed by Skinner et al. (1993). Within this theory, the ion transport is described as a three-step mechanism consisting in an ion that couples with a channel, passes through the channel, and then is released on the opposite side of the membrane. These three processes are described using the statistical rate theory approach (Ward, 1977; Ward et al., 1982). This picture seems to be appropriate when the channel is considered as a stable structure that permanently spans the lipid bilayer.

For a black lipid bilayer, when the channel or pore can be thought as caused by short-lived water channels induced by thermal fluctuations, it seems more appropriate to describe the ion-pairing reaction through an additional kinetic process, as the simultaneous presence of an ion and a pore across which it can diffuse is needed. Neglecting the detail of the microscopic interactions, the water pores in presence or absence of an ion can be simply defined as "quasi-particles" the thermodynamic properties of which can be completely described and properly defined as an electrochemical potential. Such a scheme provides a good approximation to describe the current-voltage relationships in the different systems we have investigated, and under different conditions, it can be viewed as an extension with respect to the original approach proposed by Skinner et al. (1993) toward simple bilayer systems.

The results presented in this work, concerning the electrical conduction in single lipid bilayers and mixed bilayers under all the experimental conditions used here and over an extended range of electrical potentials in which deviations from an ohmic behavior occur, can be accounted for by the current-voltage relationships we have derived. The phenomenology of these events depends on three different parameters, i.e., the two rate constants that govern the ion exchange at the membrane interfaces and rate constant across the pore. These quantities have been evaluated in the case of K^+ and Cl^- ions in different membrane bilayers as a function of temperature and ion concentration. The integration of such results into the general understanding of ion transport in lipid bilayers governed by kinetic processes is the central aim of this work.

THEORETICAL CONSIDERATIONS

Review of the statistical rate approach of the Skinner model

We proceed now to a brief summary of the Skinner model. On the basis of the statistical rate approach proposed by Ward (1977) and Ward et al. (1982), Skinner et al. (1993) recently derived an expression to describe the kinetics of the ionic transport across a membrane. The overall permeation model consists of three independent steps, and each gives rise to an ionic flux, i.e., from the external medium to the membrane pore, across the membrane pore, and from the membrane pore to the inner medium, respectively. In the steady-state condition, for each step, according to the sta-

tistical rate approach (Skinner et al., 1993), the fluxes J_i, J_{ch}, J_e through the internal interface, the external interface, and the pore, respectively, can be written as

$$J_i = K_i\left\{\frac{\beta_i C_i \exp(\phi^i)}{C_p^i \exp(\phi_p^i)} - \frac{C_p^i \exp(\phi_p^i)}{\beta_i C_i \exp(\phi^i)}\right\}$$

$$J_{ch} = K_{ch}\left\{\frac{C_p^i \exp(\phi_p^i)}{C_p^e \exp(\phi_p^e)} - \frac{C_p^e \exp(\phi_p^e)}{C_p^i \exp(\phi_p^i)}\right\} \quad (1)$$

$$J_e = K_e\left\{\frac{C_p^e \exp(\phi_p^e)}{\beta_e C_e \exp(\phi^e)} - \frac{\beta_e C_e \exp(\phi^e)}{C_p^e \exp(\phi_p^e)}\right\}$$

in which ϕ^i, ϕ^e and C_i, C_e are the reduced electrical potentials and the ionic concentrations, respectively, in the inner (index i) and outer (index e) external bulk medium on each side of the membrane, and β_i and β_e are the ion partition coefficients. The corresponding quantities ϕ_p^i, ϕ_p^e and C_p^i, C_p^e are the reduced potentials and the ionic concentrations at the membrane surface on the inner side (superscript i) and at the membrane surface on the outer side (superscript e). K_i, K_{ch}, and K_e are the equilibrium exchange rates per unit area of the interface from the inner medium to the bilayer, across the bilayer (the pore), and from the bilayer to the external medium, respectively. Finally, at each position j, the reduced potential ϕ^j is defined as

$$\phi^j = \frac{zF}{RT} V^j$$

in which z is the ion valence, R is the gas constant, T is the absolute temperature, F is the Faraday constant ($F \approx 96{,}500$ C/mol), and V^j is the applied voltage.

In the steady state condition, the fluxes (Eq. 1) must be equal. This yields, taking the reference potential as that of the external medium as usually ($\phi^i - \phi^e = \phi^i = \phi$), the following set of equations

$$\begin{cases} \dfrac{x}{y} - \dfrac{y}{x} = \dfrac{K_i}{K_{ch}}\left(\dfrac{\beta_i C_i \exp(\phi)}{x} - \dfrac{x}{\beta_i C_i \exp(\phi)}\right) \\ \dfrac{x}{y} - \dfrac{y}{x} = \dfrac{K_e}{K_{ch}}\left(\dfrac{y}{\beta_e C_e} - \dfrac{\beta_e C_e}{y}\right) \end{cases} \quad (2)$$

in which $x = C_p^i \exp(\phi_p^i)$ and $y = C_p^e \exp(\phi_p^e)$.

Skinner et al. (1993) obtained an analytical solution of the above system (Eq. 2) in two particular cases, i.e., when the equilibrium exists at the interfaces (the rates at the interfaces are infinity, $K_i = K_e \to \infty$), yielding a current density given by

$$I = zFK_{ch}\left(\frac{\beta_i C_i}{\beta_e C_e}\exp(\phi) - \frac{\beta_e C_e}{\beta_i C_i}\exp(-\phi)\right) \quad (3)$$

and when the equilibrium exchange rates are the same for all the three fluxes, i.e., $K_i = K_{ch} = K_e$, yielding a current density given by

$$I = zFK_{ch}\left(\left(\frac{\beta_i C_i}{\beta_e C_e}\exp(\phi)\right)^{1/3} - \left(\frac{\beta_e C_e}{\beta_i C_i}\exp(-\phi)\right)^{1/3}\right) \quad (4)$$

Typical dependencies in these two particular cases are shown in Fig. 1 in which the current-voltage relationships (I-V relationships) are calculated from Eqs. 3 and 4 for different values of the ratio $k = \beta_i C_i/\beta_e C_e$ between the ionic concentration in the inner and outer medium. As can be seen, the I-V curves show a marked nonlinear behavior that becomes more linear as a symmetrical condition ($k = 1$) is approached. As pointed out by Skinner et al. (1993), the nonlinear I-V curves can be obtained even when the inner and outer concentrations are the same and the system undergoes a symmetrical behavior ($\beta_i = \beta_e$), whereas in regions around the reversal potential, the curves are always almost linear and the conductance remains approximately constant.

Although the analytical solutions proposed by Skinner et al. (1993) deal with frequently encountered cases and represent a relevant description of the ionic transport across confined systems, in the general case, the numerical solution of the nonlinear system proposed by Skinner et al. (1993) (Eq. 2) is with no additional assumptions difficult, and it was never studied in detail. In the following, we have attempted to find an equation for the flux J that is surely simpler to be handled than Eq. 2 and allows to be solved numerically. To this end (see Appendix), Eq. 2 can be rearranged to give the ionic flux in an implicit form according to Eq. 5

$$\sinh(V_{eff})\left\{\sqrt{1+\left(\frac{J}{2K_i}\right)^2}\sqrt{1+\left(\frac{J}{2K_e}\right)^2} + \frac{J^2}{4K_iK_e}\right\} - \cosh(V_{eff})\left\{\frac{J}{2K_e}\sqrt{1+\left(\frac{J}{2K_i}\right)^2} + \frac{J}{2K_i}\sqrt{1+\left(\frac{J}{2K_e}\right)^2}\right\} = \frac{J}{2K_{ch}} \quad (5)$$

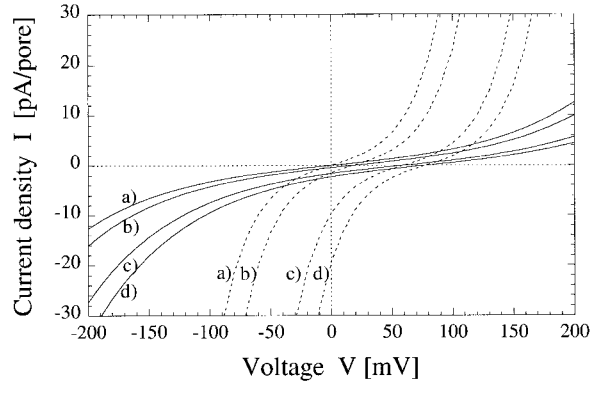

FIGURE 1 I-V relationships calculated from Eq. 3 (*dotted lines*) and Eq. 4 (*solid lines*) in the particular case $K_{ch} = 10^{-5}$ pmol/s for different values of the ratio $k = \beta_i C_i/\beta_e C_e$: (*a*) $k = 1$; (*b*) $k = 0.5$; (*c*) $k = 0.1$; (*d*) $k = 0.05$. The temperature is 300 K and $z = 1$.

in which $V_{eff} = \phi + \ln(\beta_i C_i/\beta_e C_e)$. This equation, that obviously reduces to Eq. 3 in the limit $K_i = K_e \to \infty$ when equilibrium exists on both sides of the bilayer or to Eq. 4 when the equilibrium exchange rates are the same for all the three fluxes, can be solved numerically and represents the solution of the Skinner model in the general case. Moreover, Eq. 5 provides an analytical solution in an additional case with respect to those reported by Skinner et al. (1993) when the system behaves unsymmetrically, equilibrium exists on one side of the membrane (for example $K_e \to \infty$), and the pore constant K_{ch} differs from the exchange rate on the other side of the membrane ($K_{ch} \neq K_i$). In this case, the current density is given by

$$I = \frac{2zFK_{ch}\sinh(V_{eff})}{\sqrt{1 + 2\frac{K_{ch}}{K_i}\cosh(V_{eff}) + \left(\frac{K_{ch}}{K_i}\right)^2}} \quad (6)$$

Finally, when the constant rates at the interfaces are equal, i.e., $k = K_i = K_e$, but different from the rate constant K_{ch}, the ionic flux J of Eq. 5 reduces to

$$J = 2K_{ch}\left\{\sinh(V_{eff})\left(1 + 2\left(\frac{J}{2k}\right)^2\right) - 2\cosh(V_{eff})\left(\frac{J}{2k}\right)\sqrt{1 + \left(\frac{J}{2k}\right)^2}\right\} \quad (7)$$

This equation, which can be solved numerically in an extended range of ionic concentrations and applied potentials, can be applied to phospholipid bilayers or bilayer components of a biological membrane involving the same membrane-solution interfaces. The I-V relationships calculated from Eq. 7 show a nonlinear behavior, and some typical dependencies are shown in Fig. 2 for different values of the exchange rate ranging from $k = K_i = K_e = 5 \times 10^{-5}$ to $k = K_i = K_e = 0.5$ pmol/s. All curves undergo qualitatively the same behavior, which differs from that of an ohmic regime with an increasing rate constant $k = K_i = K_e$. This feature is evidenced in the inset of Fig. 2, in which the current density, calculated at a fixed value of the applied potential, reaches a constant value as $k = K_i = K_e$ is increased.

It is noteworthy that in the general case Eq. 5 predicts that an asymptotic current density is reached for each value of the applied potential as the system becomes closer to a symmetric one. Fig. 3 shows this saturation effect in the current density calculated at a fixed value of the applied voltage as a function of the ratio K_i/K_e, in the general case $K_i \neq K_e \neq K_{ch}$. As can be seen, depending on the absolute value of the rate at the interface, the current becomes constant as the system evolves toward a symmetric bilayer ($K_i/K_e = 1$).

The case $K_i = K_e \neq K_{ch}$, which is certainly an oversimplification of the real system, is nevertheless of particular interest and deserves a more detailed analysis as it models the behavior of a symmetric pore with a rate constant different from that of the adjacent interfaces and enables us to investigate qualitative properties of model systems very similar to those studied in this work. In this case, the general equation proposed by Skinner et al. (1993) (Eq. 2) reduces to Eq. 7, the solution of which can be approximated in a closed form with the following expressions (see Appendix):

$$I = 2zFK_i\sinh \alpha V_{eff} \quad 0 \le K \le 1$$
$$I = 2zFK_i\frac{\sinh \alpha V_{eff}}{K} \quad 1 \le K \le \infty \quad (8)$$

in which the parameter α depends in a well-defined way on the ratio $K = K_i/K_{ch}$. This dependence, shown in Fig. 4, can be analytically described by two different empirical expressions, according to the range of the parameter K involved, i.e.,

$$\alpha(K) \approx \frac{1}{2}\left(1 - \frac{1}{3}K^{0.5}\right) \quad K \le 1$$
$$\alpha(K) \approx 1 - \exp\left(\ln\left(\frac{2}{3}\right)K^{0.376}\right) \quad K \ge 1 \quad (9)$$

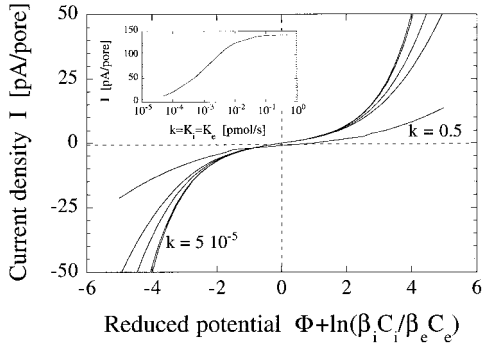

FIGURE 2 I-V relationships calculated from Eq. 7 in the particular case $K_{ch} = 10^{-5}$ pmol/s for different values of $k = K_i = K_e$ ranging from 5×10^{-5} to 0.5 pmol/s. The temperature is 300 K and $z = 1$. The *inset* shows the behavior of the current density at a fixed value of the reduced applied potential ($\phi + \ln(\beta_i C_i/\beta_e C_e) = 5$) as a function of the parameter $k = K_i = K_e$, ranging from 5×10^{-5} to 0.5 pmol/s.

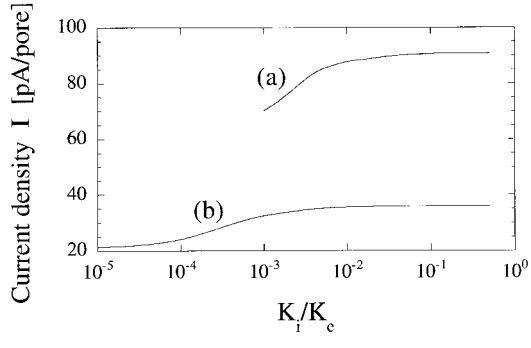

FIGURE 3 Calculated current density (Eq. 5) at a fixed value of the applied potential ($\phi + \ln(\beta_i C_i/\beta_e C_e) = 5$) as a function of the ratio K_i/K_e for different value of K_i. (*a*) $K_i = 10^{-3}$ pmol/s; (*b*) $K_i = 10^{-4}$ pmol/s. The parameter K_{ch} is assumed to be $K_{ch} = 10^{-5}$ pmol/s. The temperature is 300 K and $z = 1$. The curves show how an asymptotic value of the current density is reached, starting from an asymmetric membrane ($K_i/K_e = 10^{-5}$) toward a symmetric one ($K_i/K_e = 1$).

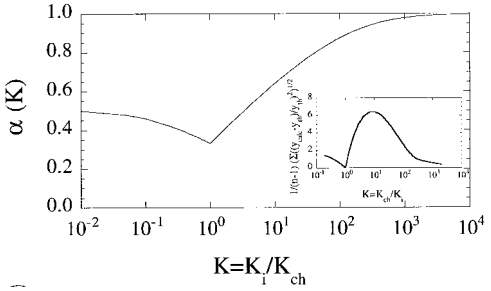

FIGURE 4 Coefficient α as a function of the ratio $K = K_i/K_{ch}$ for the particular value of the rate constant $K_{ch} = 0.2$ pmol/s. This behavior shows that in the limit $K \to 0$ and $K \to \infty$ the values of α tend to 0.5 and 1, respectively, corresponding to the explicit solution of Eq. 7. The value $K = 1$ corresponds to the value $\alpha = ⅓$, which represents the solution given in closed form by Skinner et al. (1993). The calculations has been carried out at a temperature of 300 K and for $z = 1$.

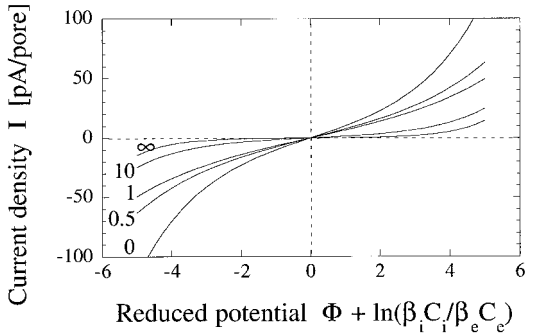

FIGURE 5 Calculated I-V relationships in the particular case $K_i = K_e \neq K_{ch}$ for different values of the ratio $K = K_i/K_{ch}$. The curves represent an analytical solution of the Skinner equation (Eq. 7) written in the form $J \sim \sinh[\alpha(K)V_{eff}]$ with $V_{eff} = \phi + \ln(\beta_i C_i/\beta_e C_e)$ and $\alpha(K)$ given in Fig. 4. The numbers on each curve refer to the value of the parameter $K = K_i/K_{ch}$. The calculations are carried out with $K_i = 10^{-4}$ pmol/s; $T = 300$ K and $z = 1$.

In this way, it is possible to derive well defined analytical expressions for the current density as solution of Eq. 7 in the case $K_i = K_e \neq K_{ch}$, which are simple enough to be readily grasped. The validity of this approximation can be seen by comparing the results from Eq. 7 and those derived from Eqs. 8 and 9. The inset of Fig. 4 shows that the normalized standard deviation between these two set of values as a function of the ratio $K = K_i/K_{ch}$ is always confined within ~6% and in particular, for values of $K = 0$, $K = 1$, and $K = \infty$ in which an exact solution exists, the standard deviation is zero. For these values of the ratio K, Eq. 7 yields well defined analytical solutions to which correspond a value of $\alpha = ½$, ⅓, and 1, respectively, according to the expressions

$$I = 2zFK_i \sinh \frac{V_{eff}}{2} \quad K = 0$$

$$I = 2zFK_i \sinh \frac{V_{eff}}{3} \quad K = 1$$

$$I = 2zFK_{ch} \sinh V_{eff} \quad K = \infty$$

Typical behaviors of the I-V relationships calculated on the basis of Eqs. 8 and 9 are shown in Fig. 5 and show a progressive deviation from linearity as the parameter $K = K_i/K_{ch}$ decreases.

A modified version of the Skinner model

In the case of lipid bilayer membrane, the ion transport is supposed to be attributable to the formation of fluctuating water channels, i.e., short-lived water pathways that span the lipid structure that represent a mechanism of facilitated transport to overcame the potential barrier associated with the hydrophobic membrane core. The permeation and diffusion of ions involve the ion pairing with a pore, its passing through, and finally its release in the external bathing medium. The step involving the ion-pore coupling can be viewed as an additional kinetic process depending both on the ion concentration and the pore concentration that can be related to the probability of formation of the water channels.

These processes can be treated similarly to those observed in enzyme-catalyzed reactions in which some substrates must interact with an enzyme to react on an appropriate time scale. In this particular case, this means that only the simultaneous presence of a pore and an ion leads to the formation of a structure with a facilitate diffusion pathway across the membrane.

We will formulate a modified version of the Skinner et al. (1993) model on the light of this mechanism, and we will simulate the overall diffusion process as a kinetic process consisting of two different reactions, The first deals with the diffusion of an ion in a pore, and the latter deals with the ion-pore coupling at both the interfaces.

Considering the kinetic processes at the two inner and outer interfaces of the bilayer between the pores at concentrations η_p^i and η_p^e, respectively, and the ions at concentrations C_i and C_e, respectively, the following equilibria hold

$$C_i + \eta_P^i \leftrightarrow \eta_{PS}^i$$

$$\eta_{PS}^e \leftrightarrow \eta_P^e + C_e$$

and the fluxes J_i and J_e at the inner and outer interfaces can be written, according to the Skinner et al. (1993) formulation, as

$$\begin{cases} J_i = K_i\left(\dfrac{C_i \exp(\phi^i)\eta_P^i}{\eta_{PS}^i \exp(\phi_p^i)} - \dfrac{\eta_{PS}^i \exp(\phi_p^i)}{C_i \exp(\phi^i)\eta_P^i}\right) \\ J_e = K_e\left(\dfrac{\eta_{PS}^e \exp(\phi_p^e)}{C_e \exp(\phi^e)\eta_P^e} - \dfrac{C_e \exp(\phi^e)\eta_P^e}{\eta_{PS}^e \exp(\phi_p^e)}\right) \end{cases} \quad (10)$$

in which η_{PS}^i and η_{PS}^e represent the pore concentrations at the inner and outer interface, respectively, when ion-pore coupling occurred. These equations are based on the assumption that the standard contribution of the electrochemical potential does not change by passing across the inner and outer interface. That appears to be acceptable when

temperature or pressure gradients across the bilayer, as in this case, are not taken into account.

However, the processes describing the diffusion of the fluctuating defect (the pore) in the bilayer structure either in presence of an ion or not are governed by kinetic reactions with the same forward and reverse rate constants

$$\eta_P^i \leftrightarrow \eta_P^e$$

$$\eta_{PS}^i \leftrightarrow \eta_{PS}^e$$

that give rise to the fluxes

$$\begin{cases} J_P = K_{ch}\left(\dfrac{\eta_P^i}{\eta_P^e} - \dfrac{\eta_P^e}{\eta_P^i}\right) \\ J_{PS} = K_{ch}\left(\dfrac{\eta_{PS}^i \exp(\phi_p^i)}{\eta_{PS}^e \exp(\phi_p^e)} - \dfrac{\eta_{PS}^e \exp(\phi_p^e)}{\eta_{PS}^i \exp(\phi_p^i)}\right) \end{cases} \tag{11}$$

The first relation of Eq. 11 takes into account that there is a finite probability that a pore could be formed and that it spans the bilayer without the presence of any ion. Moreover, on the basis of this model, it appears reasonable that the same rate constant appears, both for the diffusion of pore-ion complex and for the diffusion of the pore alone. The second relation describes a similar mechanism when an ion is present by passing through such hydrated defects. These equations actually refer to fluxes of pore-like structures through the lipid bilayer that give rise to ionic currents when coupled to ions.

In order to simplify the theory, we have limited the number of adjustable parameters to K_i, K_e, and K_{ch}. With the additional assumption that, in the steady-state condition, the total flux of pores, both in the free state (subscript P) and in the bound state (subscript PS), must be zero, i.e.,

$$J_{PS} + J_P = 0 \tag{11a}$$

Eqs. 10 and 11, following the procedure of Skinner et al. (1993), can be rearranged to give the following implicit expression for the ionic flux, (see Appendix)

$$J = K_{ch}\left\{\sinh\frac{V_{eff}}{2}\{\sqrt{(\varphi_e+1)(\varphi_i+1)} + \sqrt{(\varphi_i-1)(\varphi_e-1)}\} - \cosh\frac{V_{eff}}{2}\{\sqrt{(\varphi_e-1)(\varphi_i+1)} + \sqrt{(\varphi_e+1)(\varphi_i-1)}\}\right\} \tag{12}$$

in which

$$\varphi_e = \sqrt{1+\left(\frac{J}{2K_e}\right)^2}$$

$$\varphi_i = \sqrt{1+\left(\frac{J}{2K_i}\right)^2}$$

and V_{eff}, as usual, is defined as

$$V_{eff} = (\phi^i - \phi^e) + \ln\left(\frac{C_i}{C_e}\right) \equiv \frac{zF}{RT}V + \ln\left(\frac{C_i}{C_e}\right)$$

This equation, which describes the behavior of the ion permeation process across the bilayer under the above stated assumptions, gives the flux through a single pore. In order to obtain the current across the bilayer investigated, Eq. 12 must be multiplied by the average number (η) of pores involved in the ion transport.

In the case $K_i = K_e \neq K_{ch}$, Eq. 12 can be solved in closed form and the current density I reduces to

$$I = \frac{2zFK_{ch}\sinh V_{eff}/2}{\sqrt{1+\left(\dfrac{K_{ch}}{K_i}\right)^2 + 2\left(\dfrac{K_{ch}}{K_i}\right)\cosh V_{eff}/2}} \tag{13}$$

This equation differs greatly from the analogous equation given by Skinner et al. (1993) (Eq. 7 or 8), and as we will show in the experiments we performed, it is able to take into account the observed behavior of the I-V curves under different conditions of the ionic concentration and the applied potentials in a very satisfactory way. Fig. 6 shows the I-V curves calculated from Eq. 13 in the special case of a symmetric system, varying the rate constant $K = K_i = K_e$ from 10^{-6} to 10^{-2} pmol/s. Also in this case, deviation from linearity occurs when the system deviates from that in which the equilibrium exchange rates are the same for the three fluxes.

Finally, a cumulative plot of the I-V relationships calculated on the basis of the Skinner model (Eqs. 4 and 5) and Skinner modified model described in this section (Eq. 13) is shown in Fig. 7 in order to compare the differences between the various expressions we have analyzed.

In the next section we will apply the above relations to describe the I-V curves we have obtained in different lipid bilayer membranes and we discuss in detail their validity.

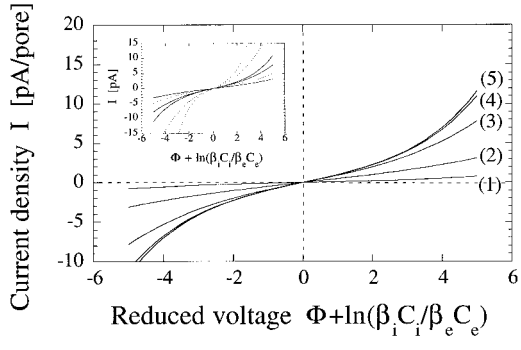

FIGURE 6 I-V relationships calculated from Eq. 13 in the particular case $K_{ch} = 10^{-5}$ pmol/s, for different values of $K_i = K_e = K$ ranging from 10^{-6} to 10^{-1} pmol/s: (*1*) $K = 10^{-6}$ pmol/s; (*2*) $K = 10^{-5}$ pmol/s; (*3*) $K = 10^{-4}$ pmol/s; (*4*) $K = 10^{-3}$ pmol/s; (*5*) $K = 10^{-2}$ pmol/s. The *inset* shows the comparison between Eq. 13, *solid lines*, and the Skinner equation (Eq. 7), *dotted lines*, in the case $K_{ch} = 10^{-5}$ pmol/s at three different values of $K_i = K_e = K$, i.e., 10^{-5}, 10^{-4}, 10^{-3} pmol/s.

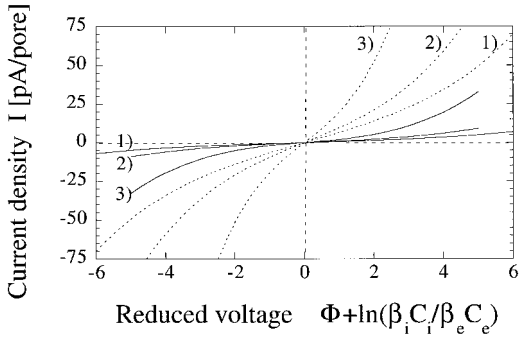

FIGURE 7 Cumulative plot of the I-V relationships based on the Skinner model and Skinner modified model for two different values of the constant rate K_{ch}. *Solid lines,* $K_{ch} = 10^{-5}$ pmol/s; *dotted lines*, $K_{ch} = 10^{-4}$ pmol/s. (*1*) analytical solution of Skinner model (Eq. 4) with $\beta_i C_i/\beta_e C_e = 1$; (*2*) numerical solution of the Skinner modified model (Eq. 13) with $K_i = 10^{-4}$ pmol/s and $K_e = 10^{-3}$ pmol/s; (*3*) numerical solution of the Skinner model (Eq. 5) with $K_i = 10^{-4}$ pmol/s and $K_e = 10^{-3}$ pmol/s.

EXPERIMENTAL

Bilayer membranes were formed at the tip of a patch-clamp pipette using the tip-dip technique described by Coronado and Latorre (1983; Coronado, 1985). After immersion of a glass pipette within the electrolyte solution (0.01 M KCl, 10 mM Hepes-Tris, pH 7.5) contained in the measuring cell, a phospholipid monolayer was formed at the air-water interface by spreading 20 μl of a 1 mg/ml solution of the lipid investigated, which was dissolved in chloroform. The so-called Langmuir monolayer forms spontaneously as the solvent spreads and evaporates.

The thermodynamic state of the lipid assembly at the interface was controlled by the determination of a surface pressure-area isotherm obtained by means of a Langmuir trough. For all the systems studied, the isotherms we have measured show the existence of at least four monolayer phases, ranging from the gas to the solid state, passing through the liquid expanded and the liquid condensed phases. In this latter phase, the tails of phospholipids are almost entirely in transconformations, and the head groups are completely ordered, thus suggesting that the packing is similar to that of a three-dimensional solid.

After the evaporation of the solvent from the surface of the solution, as the interface is progressively reduced until a liquid-condensed phase is reached (evidence is given by the surface area per polar head group), the pipette is moved out into the air and back into the solution to which corresponds the formation of a lipid bilayer at the tip of the pipette. Generally, two or three trials were performed because a gigaseal could be formed. The formation of the seal that gives rise to the bilayer structure was ascertained by the change in the electrical resistance that takes place during the movements of the pipette.

To insure that the seal was actually because of the formation of a bilayer, the seal was checked by the recording of alamethicin channels (Suarez-Isla et al., 1983). In this case, the pipette was filled with 0.2 M KCl, 5 mM Hepes-Tris, pH 7.5, containing 100 ng/ml alamethicin. The same buffer without the protein was used to form the phospholipid monolayer. The electrical current through alamethicin channels recorded by means of the standard patch-clamp technique is shown in Fig. 8 and reveals the typical behavior generally observed in planar single bilayer structures.

Lipids used in this investigation were dimyristoylphosphatidyl ethanolamine (DMPE), dimyristoylphosphatidylcholine (DMPC), and phosphatidic acid dipalmitoyl. These products were obtained from Sigma and used without any additional purification.

All the measurements were carried out in the temperature range from 5 to 35°C within 0.5°C. Movement of the pipette was obtained in a reproducible manner by means of a step-by-step dipper of the Langmuir-Blodget trough.

The lipid bilayer separates two aqueous phases conventionally defined as inner (the aqueous phase within the pipette) and outer medium (the external electrolyte solution). Pipettes were filled with an KCl electrolyte solution at different molarities between 0.02 and 0.2 M, whereas the outer medium was maintained at an ionic concentration of 0.02 M KCl.

To measure the electrical currents produced by KCl gradients under the influence of an external electrical field (up to $\pm$ 200 mV), the bilayers were formed with both the aqueous phases at an identical concentration, and the electrolyte concentration in the electrode pipette compartment was then varied by the addition of more concentrated salt solutions. The inner medium is the one to which a voltage is connected to the bilayer through an Ag/AgCl electrode, whereas the outer medium is connected to the ground through a second Ag/AgCl electrode. The voltage was applied to the electrode inside the pipette while the external electrode was grounded through the current amplifier.

Pipettes, made of hard glass capillaries (KG 33), were prepared immediately before use by means of vertical pipette puller (Model PP-83, Narishige, Japan) using the standard two-pull method. The heater current was adjusted to produce pipettes with a tip diameter in the range of 5–10 μm yielding an open tip resistance when measured in 0.02 M KCl, 10 mM Hepes-Tris, pH 7.5, of the order of 5–10 MΩ.

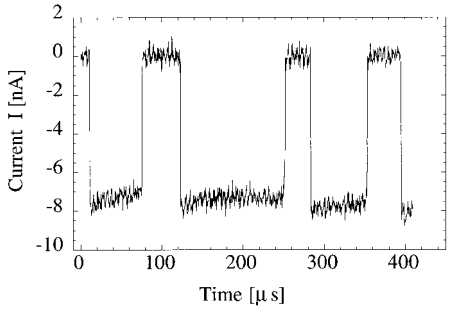

FIGURE 8 Record of current through alamethicin channels.

RESULTS AND DISCUSSION

We will present here separately the results obtained for the three different systems investigated, i.e., a bilayer built up of DMPE molecules varying the concentration of KCl electrolyte solution from 0.02 to 0.2 M, a mixed bilayer built up of DMPC-DMPE mixtures at different compositions from 20:80% wt/wt to 80:20% wt/wt at a fixed ionic concentration (0.02 M KCl), and finally a mixed bilayer built up of DMPE-DPPA at a fixed composition (50:50% wt/wt) at different ionic concentrations (from 0.02–0.2 M KCl).

It must be noted that Eq. 13 gives the current density that flows through transient defects of the bilayer, whereas the measured current is related to the membrane surface selected by the area of the electrode tip we used, and consequently it depends on the average number of defects (pores) present. To make the comparison meaningful, the current in Eq. 13 must be multiplied by a factor that takes into account the surface of the bilayer investigated. However, the fitting procedure does not allow one to obtain a separate contribution of the rate constant K_{ch} from the average concentration of defects η, as well as this procedure is unable to distinguish between K_{ch} and K_i, but it only gives the ratio K_{ch}/K_i. Therefore (see Figs. 12, 15, and 18), we report the reduced rate constant ηK_{ch} and the ratio K_{ch}/K_i thus obtained from the fitting procedure we used. However, values of ηK_{ch} of the order of 10^{-6} pmol/μm^2 s as derived from our fitting procedure with a typical value of $K_{ch} = 10^{-5}$ pmol/s yield a pore density of about 10^8 pore/cm^2 in good agreement with the values generally quoted for a lipid bilayer.

I-V curves in DMPE bilayers

The I-V curves of membranes formed in different gradients of KCl concentrations showed deviations from Ohm's law. The central portions of the curves are essentially ohmic, but at higher potential, marked deviations occur. Typical I-V curves are shown in Fig. 9 at two selected temperatures for different concentrations of the external medium in the range from 0.02–0.2 M.

In the region of each curve close to zero potential, the conductance $G = (dI/dV)_{V=0}$ for all the ionic gradients investigated shows a more or less pronounced maximum in correspondence of the chain-melting phase transition temperature (Fig. 10), the magnitude of which is progressively decreased as the ionic concentration gradient is reduced from 0.2–0.02 M. This phospholipid undergoes a main transition at about $T = 30$°C. The mismatch in molecular packing between different coexisting regions (solid-like and liquid-like phases) with different structures could be invoked to justify an increase in the formation of water channels and consequently an increase in the ionic conductivity. The maximum of sodium permeability at the transition temperature of the bilayer found in different systems (Cevc, 1991) is in agreement with this hypothesis.

We will proceed now with the analysis of the observed I-V dependence on the basis of the statistical rate approach proposed by Skinner et al. (1993) and on the modified version of this theory (Eq. 13). We confine this analysis to the case $K_i = K_e \neq K_{ch}$ that represents a relevant case of practical interest. For all the systems we considered, the Skinner model, Eq. 7 or equivalently Eq. 8, predicts deviation from an ohmic behavior more marked than that observed experimentally, whereas the modified version of the Skinner model is able to describe accurately the dependence of the current density upon the whole voltage range investigated. A typical example is shown in Fig. 11, in which we compare the experimental data for DMPE bilayer at the temperature of 5°C and ionic concentration of 0.1 M with the expected values on the basis of Eq. 7 (Skinner model) and Eq. 13 (modified Skinner model). As can be seen, Eq. 7 predicts a more marked deviation from an ohmic behavior and a conductance lower than that observed experimentally.

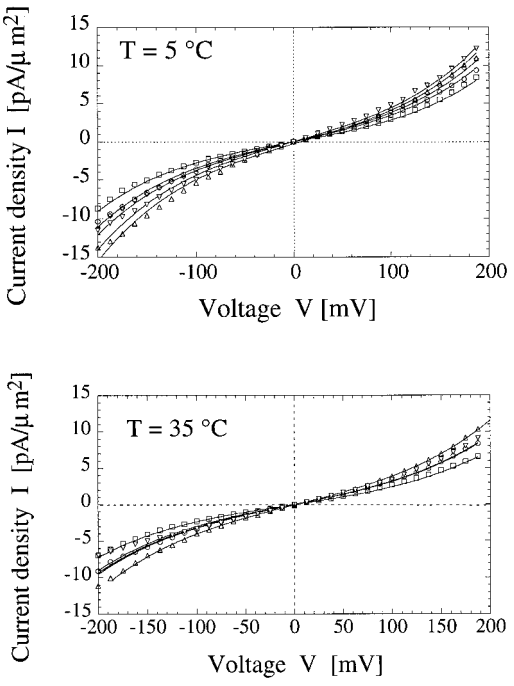

FIGURE 9 I-V curves of DMPE bilayer at two different temperatures for different values of the ionic concentration from 0.02–0.2 M KCl. (▽) 0.2 M; (△) 0.1 M; (☆) 0.075 M; (○) 0.05 M; (□) 0.02 M.

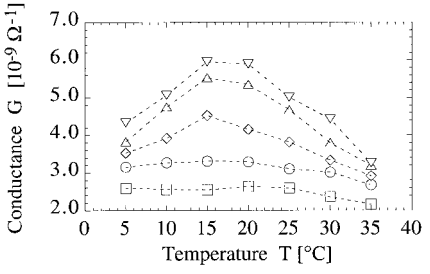

FIGURE 10 Conductance G in the ohmic region of the I-V curves of the DMPE bilayer as a function of temperature, at different ionic concentration from 0.02–0.2 M KCl. (▽) 0.2 M; (△) 0.1 M; (☆) 0.075 M; (○) 0.05 M; (□) 0.02 M.

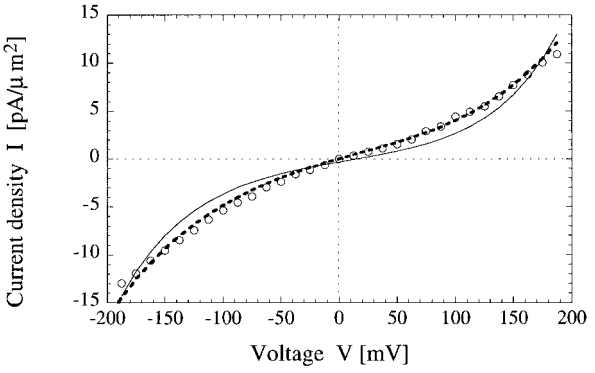

FIGURE 11 I-V curve of DMPE bilayer at the temperature of 5°C and ionic concentration of 0.1 M, compared with the values calculated according to Eq. 7 (*solid line*, Skinner model) and to Eq. 13 (*dotted line*, modified Skinner model). Both of the models depend on four free parameters, the values of which, derived from the fitting procedure, are: Eq. 13, K^+ ion, ηK_{ch} = 0.085 pmol/μm^2 s and K_{ch}/K_i = 0.95; Cl^- ion, ηK_{ch} = 0.075 pmol/μm^2 s and K_{ch}/K_i = 1.0, and Eq. 7, K^+ ion, ηK_{ch} = 0.15 pmol/μm^2 s and $K_e = K_i$ = 0.75; Cl^- ion, ηK_{ch} = 0.095 pmol/μm^2 s and $K_e = K_i$ = 0.88. As can be seen, Eq. 13 gives a very good agreement over the whole potential interval investigated.

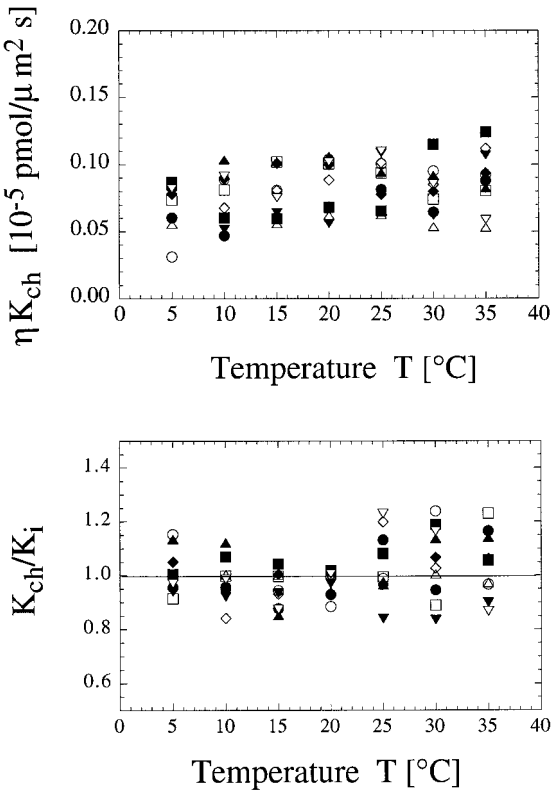

FIGURE 12 Parameters ηK_{ch} and K_{ch}/K_i deduced from a nonlinear least-squares fit of Eq. 13 to the observed I-V curves of DMPE bilayer as a function of temperature for the various ionic concentrations investigated. *Solid symbols* refer to K^+ ions: (●) 0.02 M KCl; (■) 0.075 M KCl; (▲) 0.05 M KCl; (♦) 0.1 M KCl; (▼) 0.2 M KCl. *Open symbols* refer to Cl^- ions: (○) 0.02 M KCl; (□) 0.075 M KCl; (△) 0.05 M KCl; (☆) 0.1 M KCl; (▽) 0.2 M KCl.

On the contrary, with the same number of adjustable parameters, Eq. 13 is in good agreement with the measured values.

In order to gain additional information on the behavior of the conducting pores, we have analyzed the I-V curves on the basis of Eq. 13 written for the two ionic species present in the system (K^+ and Cl^-), and the parameters ηK_{ch} and $K_{ch}/K_i = K_{ch}/K_e$ have been derived by a nonlinear least-squares minimization. The results are shown in Fig. 12 as a function of temperature for the different ionic concentrations investigated (solid symbols refer to K^+ ions and open symbols refer to Cl^- ions). As can be seen, since the uncertainties on each parameter are rather large, no particular behavior as a function of temperature can be found. Nevertheless, it must be noted that the ratio K_{ch}/K_i is approximately one both for K^+ and Cl^- ions, suggesting that the whole process occurs essentially with a single rate constant (the constant K_{ch}). Moreover this parameter is largely independent of temperature, and the pore behaves similarly with respect to K^+ and Cl^- ions.

On the basis of the results shown in Fig. 12, an additional analysis of the data has been carried out considering $K_{ch} = K_i$, thus reducing the number of free parameters to two only. It must be noted that, under the condition $K_{ch} = K_i$, Eq. 13 simplifies to

$$I = 2zFK_{ch}\sinh\left(\frac{V_{eff}}{4}\right) \tag{14}$$

No substantial improvement can be found in the behavior of K_{ch} for both K^+ and Cl^- ions as a function of temperature.

In the limit of low potential ϕ, the conductance G should reflect the behavior of the rate K_{ch}. This feature is not completely evidenced in the plot of Fig. 12, in which because of the large scattering of the data is not possible to obtain any dependence of K_{ch} upon temperature.

In order to ascertain if a such correlation exists, we have investigated the conductometric behavior of bilayers built up with different phospholipids (DMPC and DMPE) having the same hydrophobic portion but different polar head groups and a phase transition temperature varying from about 23–30°C, depending on phospholipid composition.

I-V curves in DMPC-DMPE mixtures

In absence of an ionic concentration gradient across the bilayer (the molarity on both sides of the bilayer is maintained constant to the value of 0.02 M), we have varied the composition of the lipid phase, doping the DMPE bilayer with DMPC molecules at different concentrations from 20–80% wt/wt. The conductivity behavior of the resulting structure is shown in Fig. 13 in which the I-V curves are plotted at two different temperatures for various lipid compositions.

The conductance in the ohmic region of the I-V curves (in the potential range up to ± 50 mV) is shown in Fig. 14 as a function of temperature at the different compositions investigated. As can be seen, the conductance of pure

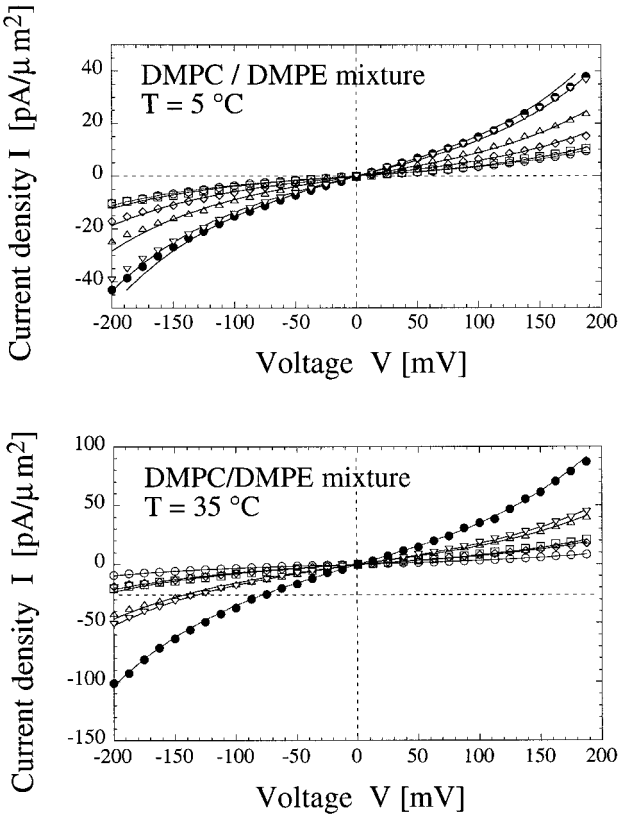

FIGURE 13 I-V curves of bilayer built up with DMPC/DMPE mixture at two different temperatures (T = 5°C and T = 35°C) and various compositions: (○) DMPE; (□) DMPC/DMPE 20:80 (wt/wt); (☆) DMPC/DMPE 40:60 (wt/wt); (△) DMPC/DMPE 60:40 (wt/wt); (▽) DMPC/DMPE 80:20 (wt/wt); (●) DMPC.

DMPC bilayer increases significantly in correspondence of the chain-melting transition temperature (T = 23°C), and this effect is progressively reduced as the concentration of DMPE increases and the transition temperature of the mixed system is shifted toward higher values (T = 30°C for DMPE). In this mixed system, the main transition temperature follows a smooth curve between 23–30°C (Cevc, 1991) that reproduces the observed behavior of the conductance.

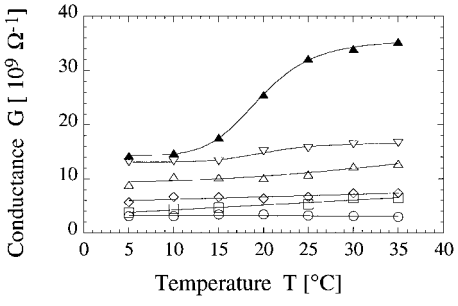

FIGURE 14 Conductance G of the mixed membrane in the ohmic region of the I-V curves as a function of temperature for various compositions: (○) DMPE; (□) DMPC/DMPE 20:80 (wt/wt); (☆) DMPC/DMPE 40:60 (wt/wt); (△) DMPC/DMPE 60:40 (wt/wt); (▽) DMPC/DMPE 80:20 (wt/wt); (●) DMPC.

The analysis of our data on the basis of the Skinner modified model (Eq. 13) furnishes the following results. In this case, the parameters ηK_{ch} and $K_{ch}/K_i = K_{ch}/K_e$, deduced from the fit of Eq. 13, behave differently in comparison with the behavior found in one-component bilayers. As can be seen in Fig. 15, the pore rate constant ηK_{ch} depends on the composition, differs for K^+ and Cl^- ions, and moreover displays a pronounced temperature dependence, whereas the ratio $K_{ch}/K_i = K_{ch}/K_e$ is approximately one for both the ions present in the system (K^+ and Cl^-), largely independent of temperature and composition. This means that, also in this case, the permeation processes could be described with a single rate constant, indicating that once the ion-pore interaction occurred, the process underlying the ion transport produces an ion to cross the bilayer.

It must be noted, however, that this analysis allows the contribution of the two ions to be separated through the different value of the K_{ch} parameter. The rate constant is significantly higher for K^+ ions than for Cl^- ions and undergoes a more marked temperature dependence.

Finally, we have analyzed the behavior of lipid mixtures in which both the hydrophobic part and the hydrophilic part have been changed.

I-V curves in DMPE-DPPA mixtures

The influence of an ion concentration gradient on the I-V curves of a bilayer built up starting from a DMPE/DPPA

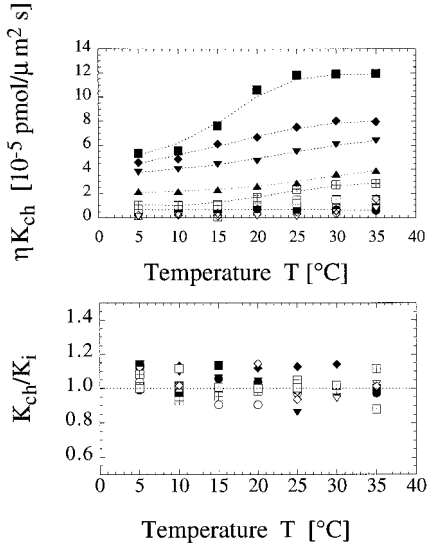

FIGURE 15 Parameters ηK_{ch} and K_{ch}/K_i deduced from a nonlinear least-squares fit of Eq. 13 to the observed I-V curves as a function of temperature for various compositions investigated. *Solid symbols* refer to K^+ ions: (●) DMPE; (□) DMPC/DMPE 20:80 (wt/wt); (▲) DMPC/DMPE 40:60 (wt/wt); (▼) DMPC/DMPE 60:40 (wt/wt); (♦) DMPC/DMPE 80:20 (wt/wt); (■) DMPC. *Open symbols* refer to Cl^- ions: (○) DMPE; (□) DMPC/DMPE 20:80 (wt/wt); (△) DMPC/DMPE 40:60 (wt/wt); (▽) DMPC/DMPE 60:40 (wt/wt); (☆) DMPC/DMPE 80:20 (wt/wt); (□) DMPC.

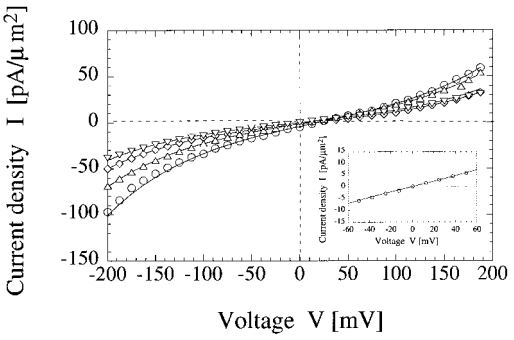

FIGURE 16 I-V curves of the mixed membrane DMPE/DPPA at the temperature of 5°C for different concentrations of KCl. (▽) 0.02 M; (☆) 0.05 M; (△) 0.075 M; (○) 0.1 M. The ion concentration of the reference side of the bilayer is maintained constant to the value of 0.02 M. The *inset* shows the ohmic part of the I-V curves in the absence of a gradient of concentration (C = 0.02 M).

mixture (50:50% wt/wt) is shown in Fig.16. The conductance G in the ohmic region of the I-V curves (Fig. 17) shows a linear increase with temperature for all the ionic concentrations investigated.

The system does not experience any phase transition in the temperature range investigated (the temperature of the main transition of DPPA is ~40°C), and as expected, no maximum level in the dependence of G upon temperature can be detected. This feature is reproduced in the temperature behavior of the rate constant ηK_{ch} obtained from the fit of Eq. 13 over the experimental data. Also in this case, the conductivity behavior over the whole potential range investigated is taken into account in a very satisfactory way by Eq. 13, and the parameters ηK_{ch} and $K_{ch}/K_i = K_{ch}/K_e$ are shown in Fig. 18. As can be seen, ηK_{ch} depends on temperature and ion concentration and moreover differs in the case of K^+ and Cl^- ions, whereas $K_{ch}/K_i = K_{ch}/K_e$ assumes as it does in the other systems investigated a value of about unity.

CONCLUSION

The results reported here show that, for all the lipid systems investigated, the modified version of the statistical rate

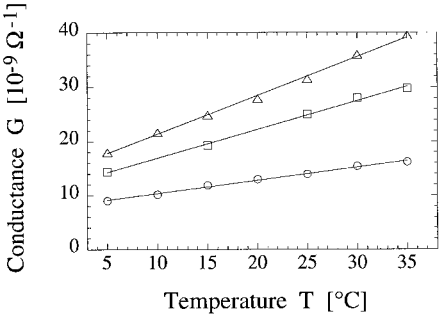

FIGURE 17 Conductance of DMPE/DPPA mixture (50:50% wt/wt) as a function of temperature in presence of different electrolyte concentrations. (○) C = 0.02 M; (□) C = 0.5 M; (△) C = 0.1 M. The concentration of the reference side of the bilayer is kept constant to the value of C = 0.02 M.

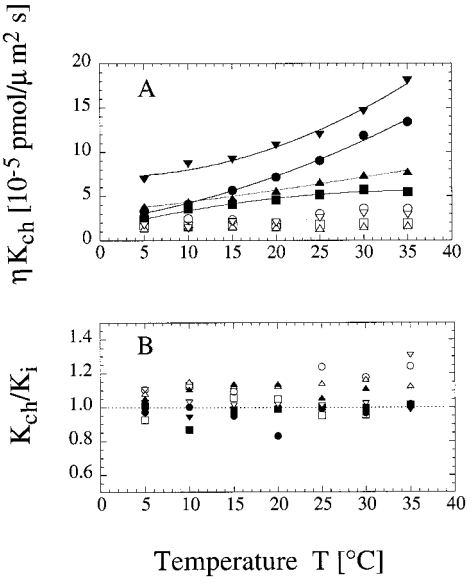

FIGURE 18 Parameters ηK_{ch} (A) and K_{ch}/K_i (B) deduced from a nonlinear least-squares fit of Eq. 13 to the observed I-V curves of DMPE/DMPA bilayers as a function of temperature for the various ionic concentrations investigated. *Solid symbols* refer to K^+ ions: (●) 0.02 M KCl; (■) 0.075 M KCl; (▲) 0.05 M KCl; (◆) 0.1 M KCl; (▼) 0.2 M KCl. *Open symbols* refer to Cl^- ions: (○) 0.02 M KCl; (□) 0.075 M KCl; (△) 0.05 M KCl; (☆) 0.1 M KCl; (▽) 0.2 M KCl.

theory approach proposed by Skinner et al. (1993) provides a very good description of the ion transport processes occurring in lipid bilayer membranes driven by a gradient of ionic concentration and applied electrical potential.

The modified version of the Skinner model, moreover, takes into account very well the deviation from an Ohmic behavior experimentally observed in the I-V characteristics, and this agreement is more marked than that found in the original model proposed by Skinner.

Our experimental findings support evidence that in the hydrophobic region of lipid bilayer, transient fluctuations (defects) are produced, giving rise to a set of pore pathways in which a passive, facilitated ion translocation occurs. This picture is in agreement with the indications of Paula et al. (1996) who pointed out that pores seem to be the dominant permeation mechanism for ion in sufficiently thin bilayers.

For the sake of completeness, it must be pointed out that other effects could be invoked to justify the deviation from linearity in the I-V curves we have observed, i.e., the density of pore could increase as the applied potential is increased as we have stated in the introduction section, or if the pore are small, the energy profile of ions passing through the pore may include a Born term, perhaps leading to a central energy barrier associated with the diffusion mechanism. All these effects could be taken into account by introducing an effective rate constant dependent on the potential. These possibilities deserve additional investigations.

In the light of the kinetic model proposed, the exchange rate constants at the interfaces with the bathing media are approximately independent of the ionic concentration, lipid

composition, and temperature, indicating that the corresponding chemical reactions do not depend on the bulk ion content. On the contrary, the pore exchange rate constant depends on the lipid composition, temperature, and moreover, the process is different for positive (K^+) and negative (Cl^-) ions. This result could suggest that also in the ionic transport within a simple bilayer without the specific components organized such as in the biological cell membrane system, the hydrophobic region exhibits a cationic selectivity.

APPENDIX

Derivation of Eq. 5

With the substitutions

$$M = \frac{\beta_i C_i \exp(\phi)}{x}; \quad N = \frac{\beta_e C_e}{y}$$

the system (2) takes the form

$$\begin{cases} \dfrac{N\beta_i C_i \exp(\phi)}{M\beta_e C_e} - \dfrac{M\beta_e C_e}{N\beta_i C_i \exp(\phi)} = \dfrac{K_i}{K_{ch}}\left(M - \dfrac{1}{M}\right) \\ \dfrac{N\beta_i C_i \exp(\phi)}{M\beta_e C_e} - \dfrac{M\beta_e C_e}{N\beta_i C_i \exp(\phi)} = \dfrac{K_i}{K_{ch}}\left(\dfrac{1}{N} - N\right) \end{cases} \tag{A.1}$$

The effective electrochemical potential can be now introduced as

$$\frac{\beta_i C_i}{\beta_e C_e}\exp(\phi) = \exp\left(\ln\left(\frac{\beta_i C_i}{\beta_e C_e}\right) + \phi\right) = \exp(V_{eff})$$

in which β_i and β_e are the partition coefficients. Substituting the corresponding expression for V_{eff} into Eq. A1, the equations can be rearranged more conveniently to give

$$\begin{cases} K_{ch}\{\sinh(V_{eff})\cosh(\ln(N) - \ln(M)) \\ \qquad + \cosh(V_{eff})\sinh(\ln(N) - \ln(M))\} = K_i \sinh(\ln(M)) \\ K_i \sinh(\ln(M)) = -K_e \sinh(\ln(N)) \end{cases}$$

From the definition of the fluxes at both the interfaces written as

$$J = 2K_i \sinh(\ln(M)) = -2K_e \sinh(\ln(N))$$

Eq. 5 follows.

Approximate solution of Eq. 7 and derivation of Eq. 8

In the case of a symmetric pore with $K_i = K_e \neq K_{ch}$, the current density is given in an implicit form by Eq. 7. However, under particular conditions, i.e., for $K_i/K_{ch} \to 1$, $K_i/K_{ch} \to 0$, $K_i/K_{ch} \to \infty$, Eq. 7 furnishes a solution in closed form and the current density is given by

$$I \approx \sinh\left(\frac{V_{eff}}{2}\right), \quad I \approx \sinh\left(\frac{V_{eff}}{3}\right), \quad I \approx \sinh(V_{eff})$$

respectively. For other values of the parameter K_i/K_{ch}, one can find a solution of the form

$$I \approx \sinh(\alpha V_{eff}) \tag{A.2}$$

with the parameter α function of the ratio K_i/K_{ch}. This dependence can be determined, to a first approximation, by equating Eq. A2 to the numerical solution of Eq. 7, and the relationship that describes the dependence of α on the value of the parameter $K = K_i/K_{ch}$ is given in Eq. 9.

Derivation of Eq. 12

In analogy with the Skinner model, the condition that in steady state regime all the fluxes must be equal yields

$$\begin{cases} K_i\left(\dfrac{C_i \exp(\phi^i)\eta_P^i}{\eta_{PS}^i \exp(\phi_p^i)} - \dfrac{\eta_{PS}^i \exp(\phi_p^i)}{C_i \exp(\phi^i)\eta_P^i}\right) \\ \qquad = K_{ch}\left(\dfrac{\eta_{PS}^i \exp(\phi_p^i)}{\eta_{PS}^e \exp(\phi_p^e)} - \dfrac{\eta_{PS}^e \exp(\phi_p^e)}{\eta_{PS}^i \exp(\phi_p^i)}\right) \\ K_e\left(\dfrac{C_e \exp(\phi^e)\eta_P^e}{\eta_{PS}^e \exp(\phi_p^e)} - \dfrac{\eta_{PS}^e \exp(\phi_p^e)}{C_e \exp(\phi^e)\eta_P^e}\right) \\ \qquad = K_{ch}\left(\dfrac{\eta_{PS}^i \exp(\phi_p^i)}{\eta_{PS}^e \exp(\phi_p^e)} - \dfrac{\eta_{PS}^e \exp(\phi_p^e)}{\eta_{PS}^i \exp(\phi_p^i)}\right) \end{cases} \tag{A.3}$$

With the condition that the fluxes of pores, both in the free state (subscript P) and in the bound state (subscript PS) must be zero

$$J_{PS} + J_P = 0$$

it follows

$$\frac{\eta_P^i}{\eta_P^e} = \frac{\eta_{PS}^e}{\eta_{PS}^i}\exp(\phi_p^e - \phi_p^i)$$

that represents the equilibrium between pores at both the interfaces in the presence and the absence of an ion. Finally, with the substitutions

$$X = \frac{C_i \exp(\phi^i)\eta_P^i}{\eta_{PS}^i \exp(\phi_p^i)}; \quad Y = \frac{C_e \exp(\phi^e)\eta_P^e}{\eta_{PS}^e \exp(\phi_p^e)}$$

Eq. A3 can be rearranged to give

$$\begin{cases} K_i\left(X - \dfrac{1}{X}\right) = K_{ch}\left(\left(\dfrac{Y\,C_i}{X\,C_e}\exp(\phi^i - \phi^e)\right)^{1/2} \right. \\ \qquad \left. - \left(\dfrac{X\,C_e}{Y\,C_i}\exp(\phi^e - \phi^i)\right)^{1/2}\right) \\ K_i\left(X - \dfrac{1}{X}\right) = K_e\left(\dfrac{1}{Y} - Y\right) \end{cases} \tag{A.4}$$

By introducing the hyperbolic functions, Eq. A4 gives

$$\begin{cases} K_i \sinh(\ln(X)) = K_{ch}\sinh\left(\dfrac{1}{2}\left(\ln\left(\dfrac{C_i}{C_e}\right)\right.\right. \\ \qquad \left.\left. + (\phi^i - \phi^e) + \ln(Y) - \ln(X)\right)\right) \\ K_i \sinh(\ln(X)) = -K_e \sinh(\ln(Y)) \end{cases}$$

and recalling that the fluxes at the interfaces are given by

$$J = 2K_i \sinh(\ln(X))$$

and by

$$J = -2K_e \sinh(\ln(Y))$$

Eq. 12 follows.

We gratefully acknowledge the Referees for a critical review of the manuscript. This work was supported by Istituto Nazionale di Fisica della Materia (INFM), Italy.

REFERENCES

Antonov, V. F., V. V. Petrov, A. A. Molnar, and D. A. Predvoditelev. 1980. The appearance of single-ion channels in unmodiofied lipid bilayer membranes at the phase transition temperature. *Nature.* 283: 585–586.

Bhowmik, B. B., and P. Nandy. 1983. Electrical conductivity of bilayer lipid membranes in electrolytic solution. *Chem. Phys. Lipids.* 34: 101–106.

Cevc, G. 1991. Polymorfism of the bilayer membranes in the ordered phase and the molecular origin of the lipid pretransition and rippled lamellae. *Biochim. Biophys. Acta.* 1062:59–69.

Cevc, G., and D. Marsh. 1987. Phospholipid Bilayers: Physical Principles and Models. J. Wiley & Sons, New York.

Chizmadzhev, Yu. A. 1988. Electric breakdown of bilayer lipid membranes. *In* Thin Lipid Film. J. B. Ivanov, editors. Marcel Dekker Inc., New York.

Coronado, R. 1985. Effect of divalent cations on the assembly of neutral and charged phospholipid bilayers in patch-recording pipettes. *Biophys. J.* 47:851–857.

Coronado, R., and R. Latorre. 1983. Phospholipid bilayers made from monolayers on batch-clamp pipettes. *Biophys. J.* 43:231–236.

Deamer, D. W., and J. W. Nichols. 1989. Proton flux mechanism in model and biological membranes. *J. Membr. Biol.* 107:91–103.

Hianik T., and V. I. Passechnik. 1995. Bilayer Lipid Membranes: Structure and Mechanical Properties. Kluwer Academic Publisher, Dordrecht.

Hladky, S. B. 1992. Kinetic analysis of lipid soluble ions and carriers. *Q. Rev. Biophys.* 25:459–475.

Kaufmann, K., and I. Silman. 1983. The induction by protons of channels through lipid bilayer membranes. *Biophys. Chem.* 18:89–99.

Jansen, M., and A. Blume. 1995. A comparative study of diffusive and osmotic water permeation across bilayer composec of phospholipids with different head groups and fatty acyl chains. *Biophys. J.* 68: 997–1008.

Lasic, D. D. 1993. Liposomes from Physics to Applications. Elsevier, Amsterdam.

Läuger P. 1976. Diffusion-limited ion flow through pores. *Biochim. Biophys. Acta.* 455:493–509.

Lawaczeck, R. 1988. Defect structures in membranes: routes for permeation of small molecules. *Ber. Bunsenges. Phys. Chem.* 92:961–963.

Levitt, D. G. 1986. Interpretation of biological ion channel flux data: reaction rate versus continuum theory. *Annu. Rev. Biophys. Biophys. Chem.* 15:29–57.

Levitt D. G. 1991. General continuum theory for multiion channels. I. Theory. *Biophys. J.* 59:271–277.

Lipowski, R., and E. Sackmann, editors. 1995. Structure and Dynamics of Membranes: from Cell to Vesicles. North-Holland, Elsevier, Amsterdam.

Nichols, J. W., and D. W. Deamer. 1980. Net proton-hydroxyl permeability of large unilamellar liposomes measured by an acid-base titration technique. *Proc. Natl. Acad. Sci. USA.* 77:2038–2042.

Owenson B., and L. R. Pratt. 1984. Monte-Carlo calculation of the molecular structure of surfactant bilayers. *J. Phys. Chem.* 88:6048–6052.

Parsegian, A. 1969. Energy of ion crossing a low dielectric membrane: solutions to four relevant electrostatic problems. *Nature.* 221:844–847.

Paula, S., A. G. Volkov, A. N. Van Hoek, T. H. Haines, and D. W. Deamer. 1996. Permeation of protons, potassium ions, and small polar molecules through phospolipid bilayers as a function of membrane thickness. *Biophys. J.* 70:339–348.

Schumaker M. F., and R. MacKinnon. 1990. A simple model for multi-ion permeation: single vacancy conduction in a simple pore model. *Biophys. J.* 58:975–984.

Skinner, F. K., C. A. Ward, and B. L. Bardakjian. 1993. Permeation in ion channels: a statistical rate theory approach. *Biophys. J.* 65:618–629.

Smith, J. R., D. R. Laver, and H. G. L. Coster. 1984. The conductance of lecithin bilayers: the dependence upon temperature. *Chem. Phys. Lipids.* 34:227–235.

Suarez-Isla, B. A., K. Wan, J. Lindstrom, and M. Montal. 1983. Single-channel recordings from purified acetylcholine receptors reconstituted in bilkayers formed at the tip of patch-pipets. *Biochemistry.* 22:2319–2323.

Vyshenskaia, T. V., and V. I. Pasechnik. 1986. Conductivity and structural transition of bilayer lipid membranes. *Biofizika.* 31:43–47.

Ward, C. A. 1977. The rate of gas absorption at a liquid interface. *J. Chem. Phys.* 67:229–235.

Ward, C. A., R. D. Findlay, and M. Rizk. 1982. Statistical rate theory of interfacial transport: I. Theoretical development. *J. Chem. Phys.* 76: 5599–5605.

Weiss, T. F. 1996. Cellular Biophysics: Transport. The MIT Press, Cambridge, MA.